Experimental quantum multimeter and one-qubit fingerprinting

Jiangfeng Du,[1,2,*] Ping Zou,[1] Xinhua Peng,[2] Daniel K. L. Oi,[3] L. C. Kwek,[4] C. H. Oh,[5] and Artur Ekert[6]
[1]*Hefei National Laboratory for Physical Sciences at Microscale and Department of Modern Physics, University of Science and Technology of China, Hefei, Anhui 230026, People's Republic of China*
[2]*Fachbereich Physik, Universität Dortmund, 44221 Dortmund, Germany*
[3]*Centre for Quantum Computation, DAMTP, University of Cambridge, Wilberforce Road, Cambridge CB3 0WA, United Kingdom*
[4]*Department of Natural Sciences, National Institute of Education, Nanyang Technological University, 1 Nanyang Walk, 637616 Singapore*
[5]*Department of Physics, National University of Singapore, 117542 Singapore*
[6]*Centre for Quantum Computation, DAMTP, University of Cambridge, Wilberforce Road, Cambridge CB3 0WA, United Kingdom*
(Received 8 April 2005; published 18 October 2006; publisher error corrected 19 October 2006)

There has been much recent effort to realize quantum devices in many different physical systems. Among them, nuclear magnetic resonance (NMR) has been the first to demonstrate nontrivial quantum algorithms with small numbers of qubits and hence is a prototype for the key ingredients needed to build quantum computers. An important building block in many quantum applications is the scattering circuit, which can be used as a quantum multimeter to perform various quantum information processing tasks directly without recourse to quantum tomography. We implement in NMR a three-qubit version of the multimeter and also demonstrate a single-qubit fingerprinting.

DOI: 10.1103/PhysRevA.74.042319 PACS number(s): 03.67.Lx, 82.56.−b

Quantum information processing exploits quantum superposition and entanglement to perform new modes of computation intrinsically different from what is possible in classical devices [1]. A particularly versatile quantum subroutine is the "scattering" circuit [2] (Fig. 1), which is used in many applications in quantum computation and communication, e.g., Kitaev's solution to the Abelian stabilizer problem [3], the analysis of quantum algorithms [4], finding approximate eigenvalues of certain Hamiltonians [5], demonstrating tomography and spectroscopy as dual forms of quantum computation [2], quantum fingerprinting [6], direct estimations of linear and nonlinear functions of a quantum state [7], and direct detection of quantum entanglement [8]. Here, we present an experimental implementation of the scattering circuit in nuclear magnetic resonance (NMR) [9], effectively creating a general purpose "quantum multimeter" and applying it to state/eigenvalue/eigenvector determination, overlap estimation, and a demonstration of quantum fingerprinting [10].

We implemented the circuit in liquid-state NMR using as qubits the three spin-$\frac{1}{2}$ carbon nuclei in a ^{13}C-labeled sample of alanine $NH_3^+-C^{\alpha}H(C^{\beta}H_3)-C'OOH$ in deuterated water. C' forms the ancilla system, which is denoted as control qubit-1. C^{α} and C^{β} form the target systems that are denoted as qubit-2 and qubit-3 (top, middle, and bottom lines in Fig. 1). With decoupling of the protons, this spin system exhibits a weakly coupled spectrum corresponding to the Hamiltonian $H=\Sigma_{i=1}^{3}\omega_i\sigma_z^i/2+\pi(J_{i,i+1}\sigma_z^i\sigma_z^{i+1}/2)$, where σ_k are rescaled Pauli matrices, $\omega_i/(2\pi)$ are Larmor frequencies, and J_{ij} are spin-spin coupling constants. The experiments were carried out at the National Institute of Sciences of Nanyang Technological University on a Bruker Avance DMX400 spectrometer with a 5 mm probe in a field of roughly 9.4 T. The frequency shifts of the other carbons with respect to the third are 12 609.6 Hz for the first and −3455.7 Hz for the second, while the coupling constants are $J_{12}=-1.2$ Hz, $J_{23}=35$ Hz, and $J_{13}=54$ Hz. Longitudinal relaxation times (T_1) for all three spins exceeded 1.5 s, while the transverse relaxation times (T_2) were at least 420 ms.

Experimentally, the device is implemented in three steps.

(i) Preparation of input $|0\rangle\langle 0|\otimes\varrho_a\otimes\varrho_b$. As standard, the density matrix of a qubit is represented by its Bloch vector $\vec{r}$ and the Pauli matrices $\vec{\sigma}=\{\sigma_x,\sigma_y,\sigma_z\}$ as $\rho=(I+\vec{r}\cdot\vec{\sigma})/2$ (where I is the unit matrix). The length of the Bloch vector r is a measure of purity (pure $r=1$ to maximally mixed $r=0$). We first use the spatial labeling method [11] to prepare the

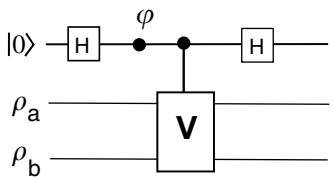

FIG. 1. Scattering circuit. The top line represents an ancilla qubit, initialized in the state $|0\rangle$, acting as a "probe particle." The lower two lines represent two physical systems of interest. The Hadamard gate (H) transforms $|b\rangle\mapsto(|0\rangle+(-1)^b|1\rangle)/\sqrt{2}$, $b\in\{0,1\}$, and the phase-shift gate $\varphi=e^{-i\varphi\sigma_z/2}$ rotates the ancilla qubit by the angle φ about the z axis of the Bloch sphere. The controlled-V operation is the controlled-SWAP gate (also called quantum Fredkin gate), which acts trivially if the ancilla qubit is in state $|0\rangle$, and swaps the two states of the lower systems if the ancilla qubit is in the state $|1\rangle$, i.e., $|1\rangle|\alpha\rangle_a|\beta\rangle_b\overset{V}{\mapsto}|1\rangle|\beta\rangle_a|\alpha\rangle_b$, $\forall|\alpha\rangle$, $|\beta\rangle$. Finally, a measurement of the ancilla in the $\{|0\rangle, |1\rangle\}$ basis has outcome probabilities $P_{0,1}=(1\pm\cos\varphi\,\mathrm{Tr}[\varrho_a\varrho_b])/2$, respectively for input density operators $\varrho_a\otimes\varrho_b$. Their difference, $|P_0-P_1|=|\cos\varphi\,\mathrm{Tr}[\rho_a\rho_b]|$, is easily measured in an NMR interferometer, and is the visibility $v=\mathrm{Tr}[\varrho_a\varrho_b]$ when $\varphi=0$.

*Electronic address: djf@ustc.edu.cn

effective pure state $\rho_{pp}=|000\rangle\langle 000|=(I+\sigma_z^1)/2\otimes(I+\sigma_z^2)/2\otimes(I+\sigma_z^3)/2$. To prepare arbitrary mixed states ϱ_a and ϱ_b from ρ_{pp}, we adopt similar methods as in previous experiments where both unitary operators and nonunitary operators were used [12].

For example, to create the mixed states $\varrho_a\otimes\varrho_b=(I+\sqrt{2}\sigma_z^2)/2\otimes(I+\sigma_x^3)/2$ from ρ_{pp}, two spin-selective radiofrequency (rf) pulses, $e^{-i\pi\sigma_x^2/8}$ and $e^{-i\pi\sigma_x^3/6}$, are applied on qubit-2 and qubit-3, respectively, transforming $(I+\sigma_z^2)/2\otimes(I+\sigma_z^3)/2\mapsto[I-\sqrt{2}(\sigma_y^2-\sigma_z^2)]/2\otimes(I-\sqrt{3}\sigma_y^3+\sigma_z^3)/2$. A pulsed field gradient (PFG) in the z axis is then applied to dephase off-diagonal elements of the density matrix leading to the state $(I+\sqrt{2}\sigma_z^2)/2\otimes(I+\sigma_z^3)/2$. Finally, another spin-selective rf pulse $e^{-i\pi\sigma_y^3/4}$ prepares the desired state. All spin-selective pulses were Gaussian-shaped and had the same pulse duration 0.866 ms, with the rotation magnitude determined by the pulse power.

(ii) Running the circuit. The single qubit gates H and φ gate have been realized in NMR [9]. The three-qubit Fredkin gate [13] can be decomposed into one- and two-qubit gates [14–17]. Another method is to directly construct multiqubit quantum gates by using low-power rf pulses on a single multiplet component [transition-selective excitation (TSE)] [18].

We implement the circuit by the pulse sequence (L-R),

$$R_\varphi^1\left(\frac{\pi}{2}\right)-TP1-TP2-TP3-R_\delta^1\left(\frac{\pi}{2}\right), \tag{1}$$

where $R_\varphi^1(\pi/2)=e^{-i\pi(\sigma_x\cos\varphi+\sigma_y\sin\varphi)/4}$ denotes a $\pi/2$ selective pulse that acts on qubit-1 about the axis $\hat{x}\cos\varphi+\hat{y}\sin\varphi$, combining the first Hadamard and the φ gate in Fig. 1. The next three transition pulses perform a modified Fredkin gate with a nontrivial phase factor [19]. The duration of each Gaussian-shaped TSE pulse was 73.5 ms for sufficient selectivity in the frequency domain (for detailed analysis of TSE pulses, see [20]).

(iii) Measure the "probe" qubit-1. The final reduced density matrix of qubit-1 is

$$\varrho_1=\begin{pmatrix}\varrho_{00}&\varrho_{01}\\ \varrho_{10}&\varrho_{11}\end{pmatrix}=(\varrho_{01}+\varrho_{10})\frac{\sigma_x^1}{2}+(\varrho_{01}-\varrho_{10})i\frac{\sigma_y^1}{2}+(\varrho_{00}-\varrho_{11})\frac{\sigma_z^1}{2}+(\varrho_{00}+\varrho_{11})\frac{I}{2}. \tag{2}$$

We obtain $|P_0-P_1|$ when the coefficient of $\sigma_z^1/2$ is measured by first applying a PFG to remove the nondiagonal part of the density matrix, and then a pulse $R_{\pi/2}^1(\pi/2)$. The state of qubit-1 is now $(\varrho_{00}-\varrho_{11})\sigma_x^1/2+(\varrho_{00}+\varrho_{11})I/2$. Since the identity matrix in NMR is not observable, the integral area of peaks of qubit-1 is now proportional to $(\varrho_{00}-\varrho_{11})=\cos\varphi\,\mathrm{Tr}[\varrho_a\varrho_b]$. Practically, this is measured by integrating the entire multiplet and adding together the signals arising from the four components of qubit-1. Figure 2(a) compares interference patterns from theory [7] and experiment, for both pure and mixed states.

We now use the scattering circuit as a quantum multimeter and perform quantum fingerprinting by suitable choice of input states $\varrho_a\otimes\varrho_b$. A multimeter can be used to estimate

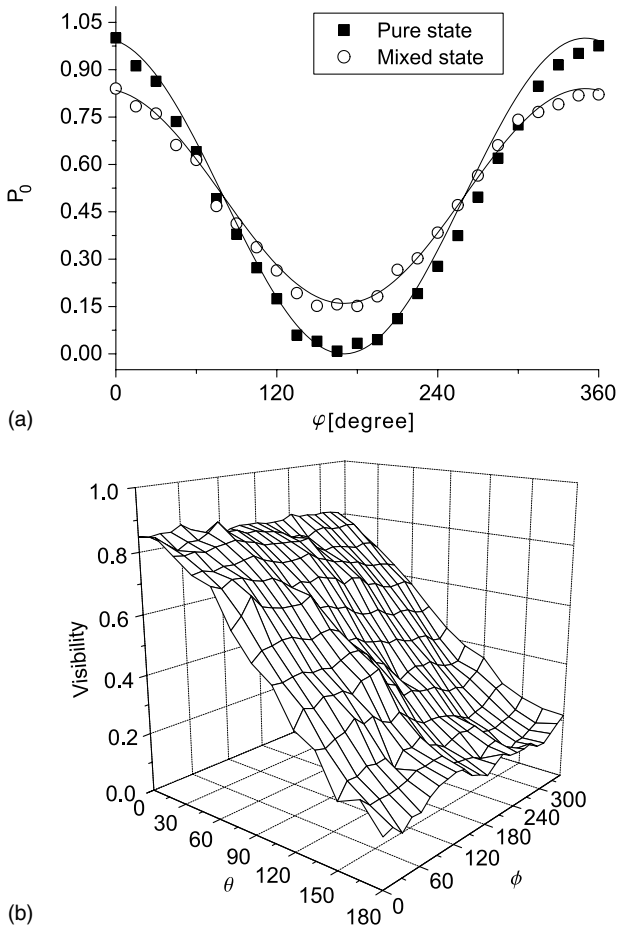

FIG. 2. Interference patterns and visibilities. (a) The interference pattern for both pure and mixed state as a function of the angle φ of phase gate. The boxes and circles are experimental results when both input states $\{\varrho_a,\varrho_b\}$ are equal to $(I+\sigma_z)/2$ or $I/2+\sqrt{3}\sigma_z/4$, respectively. The solid and dotted curves correspond to the theoretical interference pattern $P_0=(1+\cos\varphi\,\mathrm{Tr}[\varrho_a\varrho_b])/2$. Note that the additional phase factor induced by the three TSE pulses has no effect on the interference pattern since both Bloch vectors of the inputs $\varrho_{a,b}$ are in the z direction; the angle δ of the last pulse in Eq. (1) is set to $\pi/2$. It can be seen that the phase shift due to the SWAP operator is zero, and the visibility decreases when the input state changes from being pure ($r=1$) to mixed ($r=\sqrt{3}/2$). (b) The experimental visibilities $\mathrm{Tr}[\varrho_a\varrho_b]$ measured when the pure state $\varrho_a(\theta,\phi)$ is scanned over the Bloch sphere by changing the angle θ and ϕ. The second input state, ϱ_b, is fixed as $\varrho_b=I/2+\sqrt{2}\sigma_z/4$. The experimentally determined eigenvalues are $\{0.833, 0.182\}$ for eigenvectors $|0\rangle$ and $|1\rangle$, respectively, which compare well with the ideal results, $\{1/2\pm\sqrt{2}/4\}=\{0.854,0.146\}$.

the properties of a quantum state, or compare two quantum states, which are basic quantum processing tasks. Quantum fingerprinting is a proof-in-principle of an exponential quantum/classical gap for the equality problem in the simultaneous message passing model of communication complexity [6,10,21]. To cancel the effect of the additional phase factor induced by three TSE pulses, we set $\varphi=\pi/4$ and $\delta=3\pi/2$ in Eq. (1).

Multimeter for an unknown state. We detect an unknown qubit state of ϱ_b and find its eigenvalue and eigenstate by

using suitable input states ϱ_a. We separately prepare three comparison states $|\psi_a\rangle\langle\psi_a| \in \{(I+\hat{\sigma}_x)/2, (I+\hat{\sigma}_y)/2, (I+\hat{\sigma}_z)/2\}$ as ϱ_a. The visibility of qubit-1 in each run contains information of the unknown state ϱ_b, which corresponds to the expectation value $\langle\sigma_{bi}\rangle=(1+r_{bi})/2$, $i=\{x,y,z\}$. Hence we can determine the density matrix ϱ_{exp} of the unknown state from these three values. Experimentally, we test many "unknown quantum" states, evaluating the overall performance using the Uhlmann fidelity [22], $\mathcal{F}[\varrho_b,\varrho_{\text{exp}}]=\text{Tr}[\sqrt{\sqrt{\varrho_b}\varrho_{\text{exp}}\sqrt{\varrho_b}}]^2$, which gave an average fidelity $\mathcal{F}[\varrho_b,\varrho_{\text{exp}}]=0.98\pm0.01$.

We can also directly estimate eigenvalues and eigenvectors of ϱ_b by scanning $\varrho_a=(I+\vec{r}_a\vec{\sigma})/2$, $\vec{r}_a=(\cos\theta\cos\phi,\cos\theta\sin\phi,\sin\theta)$, with θ ranging from 0° to 180° in 15° steps, and ϕ from 0° to 345° with 15° steps. We then measure $\text{Tr}[\varrho_a\varrho_b]$, and find the minimum and maximum. The two extrema are the eigenvalues of the unknown state ϱ_b, and the corresponding input states are its eigenvectors [Fig. 2(b)].

Multimeter for two unknown states. We can also compare two general quantum states. For pure states $\varrho_a=|\alpha\rangle\langle\alpha|$ and $\varrho_b=|\beta\rangle\langle\beta|$, the visibility of qubit-1 gives $\text{Tr}[\varrho_a\varrho_b]=|\langle\alpha|\beta\rangle|^2$, i.e., the orthogonality of $|\alpha\rangle$ and $|\beta\rangle$. For mixed states, the visibility provides a measure of overlap $\text{Tr}[\varrho_a\varrho_b]$ between ϱ_a and ϱ_b. If $\varrho_a=\varrho_b=\varrho$, then $\text{Tr}[\varrho_a\varrho_b]=\text{Tr}[\varrho]^2$, from which the purity of ϱ can be determined.

We prepare various states ϱ_a and ϱ_b as the inputs, apply the circuit, and measure their corresponding visibilities, i.e., the overlap $\text{Tr}[\varrho_a\varrho_b]=(1+r_a r_b\cos\theta)/2$, where $r_{a,b}$ are the lengths of the Bloch vectors $\vec{r}_{a,b}$, and θ is their included angle. Figure 3(a) shows the experimental results comparing two quantum states ϱ_a and ϱ_b.

We can also directly estimate the purity of a mixed state by preparing $\varrho_a=\varrho_b=(I+r\sigma_z)/2$, where $r=\cos\eta$ ($\eta=n\pi/12, n=0,1,\ldots,6$) is the purity. For each mixed state, the visibility $\text{Tr}[\rho^2]=(1+r^2)/2$ is measured from which r can easily be extracted [Fig. 3(b)].

Quantum fingerprinting. Finally, we demonstrate quantum fingerprinting [6], for which Beaudrap [10] recently defined and presented one-qubit versions that outperform all classical one-bit schemes. We implement the scheme from [10] as follows.

Alice and Bob use the same set of pure states $\{|\phi_\sigma\rangle\}_{\sigma\in S}$ as fingerprints. In particular, we set $|S|=6$ and $\{|\phi_\sigma\rangle\}_{\sigma\in S}=\{|\pm x\rangle,|\pm y\rangle,|\pm z\rangle\}$. The absolute value of the inner product of any two distinct states does not exceed $|\langle\alpha|\beta\rangle|\leq\delta=1/\sqrt{2}$.

Alice and Bob send to a referee their fingerprints, $|\phi_\alpha\rangle$ and $|\phi_\beta\rangle$ randomly selected from S, who is required to distinguish between cases $\alpha=\beta$ and $\alpha\neq\beta$. The referee puts the two states as the inputs $\{\varrho_a,\varrho_b\}$ of the scattering circuit, from which the visibility of the first qubit gives $\text{Tr}[\varrho_a\varrho_b]=|\langle\phi_\alpha|\phi_\beta\rangle|^2$. From experimental measurements of all 36 combinations, we obtain a maximum overlap of fingerprints of 0.54 when $\alpha\neq\beta$. Hence, we obtain the experimental one-side error 0.77, while the theoretical one-side error is $(1+\delta^2)/2=0.75$. The error probability is 1 for any classical one-bit fingerprinting with one-sided error.

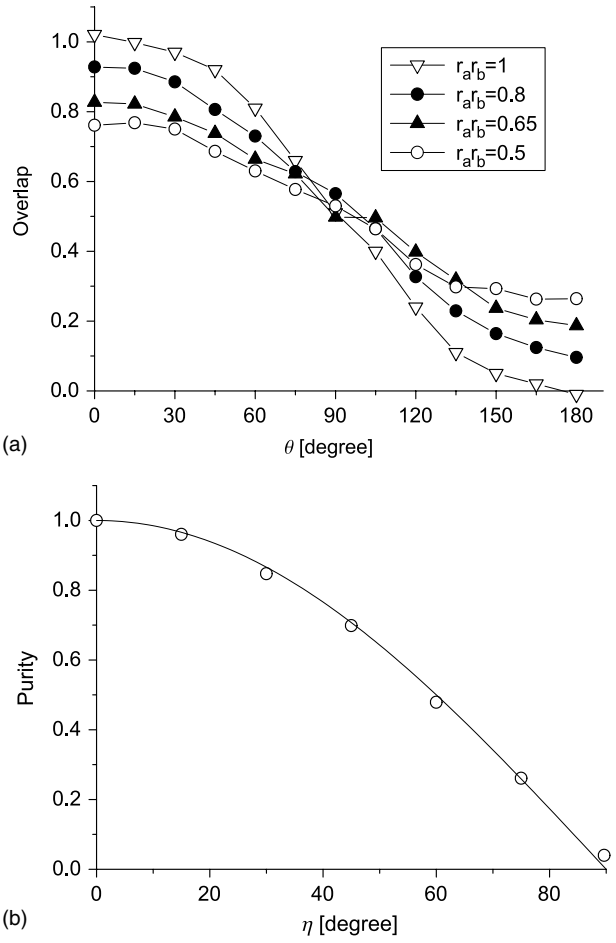

FIG. 3. Overlaps and purities. (a) Overlap as a function of θ, the angle between state vectors, with different purities r_a and r_b. Four sets of experiments are shown in the figure, distinguished by different purities of the two states $(r_a,r_b)=\{(1,1),(1,0.8),(0.81,0.81),(1,0.5)\}$. For two pure states, i.e., $r_a=r_b=1$, the results are a direct measure of orthogonality. (b) Experimental determined purity as a function of η. Note that the purity we reported here is a deviation from a pseudopure state used in NMR QIP. The experimental results (circles) compare well with theory (curve $r=\cos\eta$).

The observable errors in the experiment come from pulse imperfections, both in the TSE and spin-selective pulses, variability over time of the measurement process, and rf field inhomogeneity. Since the T_2 relaxation times of the spins varied from 0.42 to 0.8 s compared to the experiment duration of 0.23 s, the net loss of magnetization due to relaxation is not negligible. This effect has been reduced by renormalizing the integration of the spectra during the measurement stage.

In conclusion, we have used a three-spin system and liquid-state NMR to demonstrate a proof-in-principle quantum device that is a building block of many quantum applications. This versatile circuit forms a quantum multimeter with a suitable choice of input states, allowing many different tasks to be performed with the same underlying "hardware." We test several quantum computation and quantum communication applications using this quantum multimeter,

the experimental results showing good agreement with theory.

Note added. After completing this work, we became aware of the demonstration of single-qubit quantum fingerprinting using linear optics by Horn *et al.* [23].

J.D. acknowledges support from the National Fundamental Research Program (Grant No. 2001CB309300), the National Science Fundation of China, and the European Commission under Contract No. 007065. This project was also supported by Temasek Project in Quantum Information Technology, EU grants RESQ and TOPQIP, Fujitsu, CMI, EPSRC QIPIRC, and Sidney Sussex College Cambridge.

[1] D. Deutsch, Proc. R. Soc. London, Ser. A **400**, 97 (1985).
[2] C. Miquel, J. P. Paz, M. Saraceno, E. Knill, R. Laflamme, and C. Negrevergne, Nature (London) **418**, 59 (2002).
[3] A. Y. Kitaev, e-print quant-ph/9511026.
[4] R. Cleve, A. Ekert, C. Macchiavello, and M. Mosca, Proc. R. Soc. London, Ser. A **454**, 339 (1998).
[5] D. S. Abrams and S. Lloyd, Phys. Rev. Lett. **83**, 5162 (1999).
[6] H. Buhrman, R. Cleve, J. Watrous, and R. deWolf, Phys. Rev. Lett. **87**, 167902 (2001).
[7] A. Ekert *et al.*, Phys. Rev. Lett. **88**, 217901 (2002).
[8] P. Horodecki and A. Ekert, Phys. Rev. Lett. **89**, 127902 (2002).
[9] L. M. K. Vandersypen and Isaac L. Chuang, Rev. Mod. Phys. **76**, 1037 (2004).
[10] J. N. deBeaudrap, Phys. Rev. A **69**, 022307 (2004).
[11] D. G. Cory, A. F. Fahmy, and M. D. Price, Physica D **120**, 82 (1998).
[12] J. Du *et al.*, Phys. Rev. Lett. **91**, 100403 (2003).
[13] E. Fredkin and T. Toffoli, J. Theoret. Phys. **21**, 219 (1982).
[14] A. Barenco *et al.*, Phys. Rev. A **52**, 3457 (1995).
[15] H. F. Chau and F. Wilczek, Phys. Rev. Lett. **75**, 748 (1995).
[16] J. A. Smolin and D. P. Divincenzo, Phys. Rev. A **53**, 2855 (1996).
[17] M. D. Price, S. S. Somaroo, A. E. Dunlop, T. F. Havel, and D. G. Cory, Phys. Rev. A **60**, 2777 (1999).
[18] J. Du *et al.*, Phys. Rev. A **63**, 042302 (2001).
[19] F. Xue *et al.*, Chin. Phys. Lett. **19**, 1048 (2002).
[20] X. Peng *et al.*, J. Chem. Phys. **120**, 3579 (2004).
[21] S. Massar, Phys. Rev. A **71**, 012310 (2005).
[22] A. Uhlmann, Rep. Math. Phys. **9**, 273 (1976).
[23] R. T. Horn *et al.*, Phys. Rev. Lett. **95**, 150502 (2005).